Loss of choline agonism in the inner ear hair cell nicotinic acetylcholine receptor linked to the α10 subunit

Marcelo J. Moglie[1*], Irina Marcovich[1*], Jeremías Corradi[2], Agustín E. Carpaneto Freixas[1], Sofía Gallino[1], Paola V. Plazas[3], Cecilia Bouzat[2], Marcela Lipovsek[1,4§], Ana Belén Elgoyhen[1§]

[1]Instituto de Investigaciones en Ingeniería Genética y Biología Molecular "Dr. Héctor N. Torres" (INGEBI), Consejo Nacional de Investigaciones Científicas y Técnicas (CONICET), Buenos Aires, Argentina

[2]Instituto de Investigaciones Bioquímicas de Bahía Blanca, Consejo Nacional de Investigaciones Científicas y Técnicas, Buenos Aires, Argentina.

[3]Instituto de Farmacología, Facultad de Medicina, Universidad de Buenos Aires, Argentina

[4]Centre for Developmental Neurobiology, King's College London, Institute of Psychiatry, Psychology and Neuroscience, Guy's Campus, London, United Kingdom

* these authors equally contributed to this work

§ these authors equally contributed to this work

Irina Marcovich present address: Departments of Otolaryngology & Neurology, Boston Children's Hospital and Harvard Medical School, Boston, MA 02115, USA

Correspondence should be addressed to: Ana Belén Elgoyhen

Instituto de Investigaciones en Ingeniería Genética y Biología Molecular "Dr. Héctor N. Torres" (INGEBI), Consejo Nacional de Investigaciones Científicas y Técnicas (CONICET), Vuelta de Obligado 2490, 1428 Buenos Aires, Argentina.

Phone: +541147832871

Email: elgoyhen@dna.uba.ar

Abstract

The α9α10 nicotinic acetylcholine receptor (nAChR) plays a fundamental role in inner ear physiology. It mediates synaptic transmission between efferent olivocochlear fibers that descend from the brainstem and hair cells of the auditory sensory epithelium. The α9 and α10 subunits have undergone a distinct evolutionary history within the family of nAChRs. The α9α10 receptor has accumulated changes at the protein level only in mammalian vertebrates that may ultimately relate to the evolutionary history of the mammalian hearing organ. In the present work we investigated the responses of α9α10 nAChRs to choline, the metabolite of acetylcholine degradation at the synaptic cleft. Whereas choline is a full agonist of chicken α9α10 receptors it is a partial agonist of the rat receptor. Making use of the expression of α9α10 heterologous receptors, encompassing wild-type, heteromeric, homomeric, mutant, chimeric and hybrid receptors, and *in silico* molecular docking, we established that the mammalian (rat) α10 nAChR subunit underscores the reduced efficacy of choline. Moreover, we show that whereas the complementary face of the α10 subunit does not play an important role in the activation of the receptor by ACh, it is strictly required for choline responses. Thus, we propose that the evolutionary changes acquired in the mammalian α9α10 nAChR resulted in the loss of choline acting as a full agonist at the efferent synapse, without affecting the triggering of ACh responses. This may have been required to allow the post-synaptic summation needed to faithfully reproduce the high frequency activity of efferent medial olivocochlear fibers.

Introduction

The α9α10 nicotinic acetylcholine receptor (nAChR) belongs to the pentameric family of ligand-gated ion channels (Elgoyhen *et al.*, 1994, Elgoyhen *et al.*, 2001, Sgard *et al.*, 2002), each of which has a large extracellular N-terminal region, four transmembrane helices (M1–M4), and an intracellular domain. At the interface of the extracellular domains of adjacent subunits lies the orthosteric binding site, composed of a principal component or face provided by one subunit, which contributes three loops of highly conserved residues (loops A–C), and a complementary component of the adjacent subunit, which contributes three loops (loops D–F) with lower levels of sequence conservation among subunits (Thompson *et al.*, 2010). Conserved aromatic residues present within the loops participate in cation-π interactions with the agonists that are fundamental for triggering receptor gating (Karlin, 2002)

The α9α10 receptor is an atypical member of the nAChR family. Both the α9 and α10 subunits have low amino acid sequence identity when compared to other member subunits (Elgoyhen *et al.*, 1994, Elgoyhen *et al.*, 2001, Franchini & Elgoyhen, 2006, Elgoyhen *et al.*, 2009, Lipovsek *et al.*, 2012, Lipovsek *et al.*, 2014, Marcovich *et al.*, 2020) and α9α10 receptors have a baroque pharmacological profile (Rothlin *et al.*, 1999, Verbitsky *et al.*, 2000, Rothlin *et al.*, 2003). Indeed, nicotine, the canonical agonist that characterizes the receptor subfamily, does not activate α9α10 nAChRs, but blocks ACh-gated currents (Elgoyhen *et al.*, 1994, Elgoyhen *et al.*, 2001, Sgard *et al.*, 2002). Moreover, the α9α10 nAChR has a mixed nicotinic and muscarinic profile, since it is blocked by the nicotinic antagonists curare and α-bungarotoxin and the muscarinic antagonist atropine (Elgoyhen *et al.*, 1994, Elgoyhen *et al.*, 2001, Sgard *et al.*, 2002). In addition, the α9α10 receptor shares pharmacological properties with type A γ-aminobutyric acid, glycine, and type 3 serotonin receptors, also members of the pentameric family of ligand-gated ion channels (Rothlin *et al.*, 1999, Rothlin *et al.*, 2003).

The atypical features of the α9α10 receptor prompted the hypothesis that α9 and α10 subunits have undergone a distinct evolutionary history within the family of nAChRs. Using codon-based likelihood models we showed that mammalian, unlike non-mammalian α10 subunits have been under selective pressure and acquired a greater than expected number of non-synonymous amino acid substitutions in their coding region (Franchini & Elgoyhen, 2006, Elgoyhen & Franchini, 2011). Moreover, mammalian

83 specific amino acid substitutions in the α9 subunit that show an increased posterior
84 probability of functional divergence in this clade, are involved in the higher relative
85 calcium permeability of mammalian α9α10 receptors (Lipovsek *et al.*, 2014, Marcovich
86 *et al.*, 2020). Overall, these patterns of evolutionary changes at the protein level may
87 relate to the evolutionary history of the mammalian hearing organ (Marcovich *et al.*,
88 2020), which has the highest frequency sensitivity amongst vertebrate auditory systems
89 (Manley, 2000). In particular, α9α10 nAChRs mediate the synapsis, between efferent
90 fibers and sensory hair cells, that modulates sound amplification processes, including
91 the mammalian-exclusive prestin-driven somatic electromotility of outer hair cells (Katz
92 & Elgoyhen, 2014, Goutman *et al.*, 2015). Overall, the distinct evolutionary history of
93 mammalian α9α10 nAChRs resulted in differential calcium permeability, current-
94 voltage relationship and desensitization profile of α9α10 receptors across vertebrate
95 species (Lipovsek *et al.*, 2012, Lipovsek *et al.*, 2014, Marcovich *et al.*, 2020), together
96 with the loss of functional homomeric α10 receptors (Elgoyhen *et al.*, 2001, Sgard *et al.*,
97 2002, Lipovsek *et al.*, 2012) and a non-equivalent contribution of different subunit
98 interfaces to functional binding sites in mammals (Boffi *et al.*, 2017).

99 One striking feature of the pharmacology of mammalian α9α10 receptors, compared to
100 other nAChRs, is the scarcity of identified compounds capable of behaving as agonists
101 of the receptor, since most typical nicotinic agonists block rat α9α10 nAChRs
102 (Verbitsky *et al.*, 2000, Elgoyhen *et al.*, 2001). Whether these observations are related
103 to the peculiar evolutionary history of the mammalian receptor, and therefore not
104 extended to other non-mammalian α9α10 nAChRs, is still an open question. In the
105 present work we have addressed this by comparing the effects of classical nicotinic
106 agonists: nicotine, carbachol, DMPP and choline, on rat and chicken α9α10 nAChRs.
107 We report that, as for rat receptors, nicotine does not activate but blocks chicken α9α10
108 nAChRs. However, whereas choline is a partial agonist of rat α9α10 receptors, it is a
109 full agonist of chicken α9α10 receptors. Similarly, DMPP has a higher efficacy in
110 chicken receptors. Using hybrid and chimeric receptors we show that the lower
111 agonistic efficacy of choline in rat α9α10 receptors is linked to the extracellular region
112 of the mammalian α10 subunit. Most importantly, we describe that complementary
113 components of the ligand-binding site provided by the rat α10 subunit non-equivalently
114 contribute to receptor activation by ACh and choline. Thus, whereas ACh does not
115 utilize interfaces where α10 provides the complementary component to elicit maximal

116 responses, choline requires fully competent α10 interfaces for receptor activation,
117 suggesting a requirement for higher degree of ligand occupancy when choline is the
118 agonist. In line with these results, molecular docking simulations indicate that choline
119 binds at all interfaces with a different orientation with respect to that of ACh, and it
120 does so with differing frequencies depending on which subunit contributes the
121 complementary side. Overall, we propose that the loss of choline full agonism in
122 mammalian α9α10 receptors was driven by changes in the α10 subunit. This may have
123 resulted from functional selection pressure on the fine-tuning of cholinergic responses
124 within the mammalian efferent synapse.

125

126 **Materials and Methods**

127 **Expression of Recombinant Receptors in *X. laevis* oocytes**

128 For expression studies rat and chicken α9 and α10 nAChR subunits subcloned into a
129 modified pGEMHE vector were used. Capped cRNAs were *in vitro* transcribed from
130 linearized plasmid DNA templates using RiboMAX^{TM} Large Scale RNA Production
131 System (Promega, Madison, WI, USA). The maintenance of *X. laevis* and the
132 preparation and cRNA injection of stage V and VI oocytes have been described in detail
133 elsewhere (Verbitsky *et al.*, 2000). Typically, oocytes were injected with 50 nl of
134 RNase-free water containing 0.01 to 1.0 ng of cRNA (at a 1:1 molar ratio for
135 heteromeric receptors) and maintained in Barth's solution at 18°C. Electrophysiological
136 recordings were performed 2 to 6 days after cRNA injection under two-electrode
137 voltage clamp with an Oocyte Clamp OC-725B or C amplifier (Warner Instruments
138 Corp., Hamden, CT, USA). Recordings were filtered at a corner frequency of 10Hz
139 using a 900BT Tunable Active Filter (Frequency Devices Inc., Ottawa, IL, USA). Data
140 acquisition was performed using a Patch Panel PP-50 LAB/1 interphase (Warner
141 Instruments Corp., Hamden, CT, USA) at a rate of 10 points per second. Both voltage
142 and current electrodes were filled with 3 M KCl and had resistances of ~1 MΩ. Data
143 were analyzed using Clampfit from the pClamp 6.1 software. During
144 electrophysiological recordings, oocytes were continuously superfused (~15 ml/min)
145 with normal frog saline composed of: 115 mM NaCl, 2.5 mM KCl, 1.8 mM $CaCl_2$, and
146 10 mM HEPES buffer, pH 7.2. Drugs were added to the perfusion solution for
147 application. The membrane potential was clamped to -70 mV. To minimize activation
148 of the endogenous Ca^{2+} sensitive chloride current (Elgoyhen *et al.*, 2001), all

149 experiments were performed in oocytes incubated with the Ca^{2+} chelator BAPTA-AM
150 (100 μM) for 3h before electrophysiological recordings. Concentration-response curves
151 were normalized to the maximal ACh response in each oocyte. For the inhibition
152 curves, nicotine was added to the perfusion solution for 2 min before the addition of 10
153 μM ACh and then coapplied with this agonist and responses were referred to as a
154 percentage of the response to ACh. The mean and S.E.M. of peak current responses are
155 represented. Agonist concentration-response curves were iteratively fitted, using Prism
156 6 software (GraphPad Software Inc., La Jolla, CA, USA), with the equation: I/Imax =
157 $A^{nH}/(A^{nH} + EC_{50}^{nH})$, where I is the peak inward current evoked by agonist at
158 concentration A; Imax is the current evoked by the concentration of agonist eliciting a
159 maximal response; EC_{50} is the concentration of agonist inducing half-maximal current
160 response, and nH is the Hill coefficient. An equation of the same form was used to
161 analyze the concentration dependence of antagonist induced blockage. The parameters
162 derived were the concentration of antagonist producing a 50% block of the control
163 response to ACh (IC_{50}) and the associated interaction coefficient (*n*H). Data were
164 analyzed using Clampfit from the pClamp 6.1 software.

165 The α10W55T mutant subunit was produced using Quick change XL II kit (Stratagene,
166 La Jolla, CA, USA). The chimeric α10x construct was generated in two steps. First, the
167 DNA fragment encoding the α10 N-terminal domain was replaced by the DNA
168 sequence encoding the α9 N-terminal domain, by overlap-extension PCR (Horton *et al.*,
169 1989). Briefly, the DNA sequence of the α9 N-terminal domain was amplified from an
170 α9 pGEMHE construct using primers 5'GGGCGAATTAATTCGAGCTC3' and
171 5'CACCTTCACTCTCCTTCTGAAGCGCCGCGCTGCAGCCTACGTGTG3', and the
172 DNA sequence of the α10 subunit from TM1 to the C-terminal domain was amplified
173 from an α10 pSGEM construct using primers
174 5'CACACGTAGGCTGCAGCGCGGCGCTTCAGAAGGAGAGTGAAGGTG3' and
175 5'GCTATGACCATGATTACGCC3'. The chimeric subunit was amplified using the
176 DNA fragments generated in the two PCRs described above and primers
177 5'GGGCGAATTAATTCGAGCTC3' and 5'GCTATGACCATGATTACGCC3', and
178 subcloned in pSGEM vector. In a second step, conversion of both the pre TM1 and the
179 TM2-TM3 loop from the chimera to the corresponding α9 sequence was performed by
180 QuikChange Multi Site-Directed Mutagenesis kit (Stratagene) using primers
181 5'GGCATGCTCTCGGCCACCATCAGCTGGAAGACGG3' and

182 5'GGGCAGCAGGAGGTTGACGATGTAGAATGAAGAGCGGCGCTTCAG3'. All
183 mutant and chimeric subunits were confirmed by sequencing.

184

185 **Recordings from hair cells**

186 Chicken auditory organ (basilar papilla) was dissected from the temporal bone of
187 embryonic chickens (white Leghorns either sex, 17–20 d *in ovo*). The tegmentum
188 vasculosum was removed and the tectorial membrane was stripped from the basilar
189 papilla with most of the short hair cells (SHCs) still attached. This "tectorial
190 preparation" was then inverted and secured in the recording chamber by spring clips.
191 SHCs were recorded in a region 25–50% the distance from the apical (lagenar) to the
192 basal tip of the basilar papilla of the chicken. Apical turns of the organ of Corti were
193 excised from Balb/C mice of either sex between postnatal day 11 (P11) and P13,
194 (around the onset of hearing in altricial rodents). At this age OHCs are already
195 innervated by the MOC fibers (Pujol *et al.*, 1998, Simmons, 2002). The tectorial
196 membrane was removed and the organ of Corti was positioned under an insect pin
197 affixed to a cover-slip with a drop of Sylgard.

198 Basilar papilla and cochlear preparations were placed into a chamber on the stage of an
199 upright microscope (Olympus BX51WI, Center Valley, PA, USA) and used within 2 h.
200 Cells were visualized on a monitor via a water immersion objective (60×
201 magnification), differential interference contrast optics, and a CCD camera (Andor iXon
202 885, Belfast, UK). The preparation was superfused continuously at 2–3 mL per min
203 with extracellular saline solution of an ionic composition similar to that of the
204 perilymph: 144 mM NaCl, 5.8 mM KCl, 1.3 mM $CaCl_2$, 0.9 mM $MgCl_2$, 0.7 mM
205 NaH_2PO_4, 5.6 mM D-glucose and 10 mM Hepes buffer (pH 7.4). Solutions containing
206 ACh or choline were made up in this same saline and delivered by a gravity-fed
207 multichannel glass pipette (150-µm tip diameter).

208 Whole-cell, tight-seal voltage-clamp recordings were made with 1 mm borosilicate
209 glass micropipettes (WPI, Sarasota, FL, USA) ranging from 6 to 8 MΩ tip resistance.
210 Series resistance errors were not compensated for. The recording pipette contained the
211 following (in mM): 140 KCl, 3.5 $MgCl_2$, 2 $CaCl_2$, 5 EGTA, 5 HEPES, 5 mM
212 phosphocreatine-Na_2 and 2.5 Na2ATP, titrated to pH 7.2 with KOH. Osmolarity was
213 adjusted to 295 mOsM. All recordings were performed at room temperature (22–25 °C).

Electrophysiological recordings were performed using a Multiclamp 700B amplifier (Molecular Devices, San Jose, CA, USA), low-pass-filtered at 2–10 kHz, and digitized at 50 kHz via a National Instruments board. Data were acquired using WinWCP (J. Dempster, University of Strathclyde, Glasglow, Scotland). Recordings were analyzed with custom-written routines in IgorPro 6.37 (Wavemetrics, Lake Oswego, OR, USA).

Molecular modeling and docking

Homology models of the extracellular domain of the chick and rat α9α10 nAChRs were as in (Boffi *et al.*, 2017). They were created with SWISS MODEL (Schwede *et al.*, 2003, Arnold *et al.*, 2006, Bordoli *et al.*, 2009) using the monomeric structure of the human α9 subunit as the template (Protein Data Bank ID 4UY2;(Zouridakis *et al.*, 2014)). The monomeric models of these proteins were then structurally aligned to the pentameric structure of *Lymnaea stagnalis* AChBP bound to ACh (Protein Data Bank ID 3WIP; (Olsen *et al.*, 2014)) using the program STAMP (Russell & Barton, 1992) from visual molecular dynamics (Humphrey *et al.*, 1996) to obtain pentameric models with a $(\alpha9)_2(\alpha10)_3$ stoichiometry bound to ACh. Four different types of possible binding site interfaces were included: α9α9, α9α10, α10α9 and α10α10. For each interface, the first subunit forms the principal face and the second forms the complementary face. The models were energy minimized to relax steric clashes using spdbviewer (Guex & Peitsch, 1997), and were used for docking studies after deletion of ACh from the models. Using Autodock 4.2 (Morris *et al.*, 2009) choline and ACh were downloaded from PubChem and docked into each of the four types of interfaces for rat and chicken subunits. One hundred genetic algorithm runs were performed for each condition. Residues R57, R111, and R117 were set as flexible to avoid steric and/or electrostatic effects that may impair agonist docking into the binding site (Boffi *et al.*, 2017). Clustering of the results was done with Autodock based on a root-mean-square deviation cutoff of 2.0 Å. Docking results were corroborated in three different procedures. The most representative docking result was plotted with Discovery Studio Visualizer 4.5 (Dessault Systèmes BIOVIA, San Diego, 2016).

Statistical Analysis

245 Statistical analysis was performed using the software Infostat (Universidad Nacional de
246 Córdoba). The non-parametric Mann-Whitney test was used to perform comparisons
247 between two groups and Kruskal-Wallis one-way analysis of variance followed by
248 Conover's test for comparisons between multiple groups. Friedman's test was used for
249 comparisons between paired samples. Differences between samples were considered
250 significant when $p < 0.05$.

251

252 **Materials**

253 All drugs were obtained from Sigma-Aldrich (St. Louis, MO, USA). ACh, choline,
254 DMPP, carbachol and nicotine were dissolved in distilled water as stocks and stored
255 aliquoted at -20°C. BAPTA-AM was stored at -20°C as aliquots of a 100 mM solution
256 in dimethyl sulfoxide (DMSO), thawed and diluted 1000-fold into Barth's solution
257 shortly before incubation of the oocytes.

258 All experimental protocols were carried out in accordance with the National Institute of
259 Health Guide for the Care and Use of Laboratory Animals (NIH Publications No. 80-
260 23) revised 1978 and INGEBI Institutional Animal Care and Use Committee.

261

262 **Results**

263 **Cholinergic agonists show lower efficacy on rat α9α10 receptors**

264 The unique pharmacological profile of mammalian α9α10 receptors (Rothlin *et al.*,
265 1999, Verbitsky *et al.*, 2000, Rothlin *et al.*, 2003), and the observation that mammalian
266 α10 subunits have been under selection pressure (Franchini & Elgoyhen, 2006,
267 Elgoyhen & Franchini, 2011), prompted us to examine whether this baroque
268 pharmacology is recapitulated in receptors from a non-mammalian species. Nicotine,
269 the prototypic agonist of nAChRs, is an antagonist of mammalian α9α10 receptors
270 (Elgoyhen *et al.*, 1994, Elgoyhen *et al.*, 2001, Sgard *et al.*, 2002), and did not elicit
271 currents in oocytes expressing either rat or chicken α9α10 receptors. Instead, nicotine
272 acted as an antagonist of both receptors (Fig. 1A, Table 1 and (Elgoyhen *et al.*, 2001)),
273 blocking responses to 10 μM ACh in a concentration-dependent manner (rat IC_{50} = 46.3
274 ± 12.4 μM; n=6; chicken IC_{50} = 39.4 ± 3.4 μM; n=6; p=0.81, Mann-Whitney test).

275 Next, we analyzed the effect of different nAChR agonists on α9α10 receptors from the
276 two studied species. Previous work showed that ACh elicits maximal responses in both
277 rat and chicken α9α10 receptors, with similar near 10 μM EC_{50} values (Elgoyhen *et al.*,
278 2001, Lipovsek *et al.*, 2012). The cholinergic agonist carbachol elicited concentration-
279 dependent responses in oocytes expressing α9α10 receptors (Fig. 1B and Table 1) with
280 maximal responses that were 75.5 ± 5.2 % (rat, n=5) and 89.8 ± 7.0 % (chicken, n=6) of
281 the maximum response elicited by 1 mM ACh (p=0.93, Mann-Whitney test). EC_{50}
282 values for carbachol were similar for the receptors from both species: 159.3 ± 31.5 μM
283 (rat; n=5), 150.1 ± 14.8 μM (chicken; n=6); p=0.42, Mann-Whitney test. The potency of
284 carbachol was therefore nearly 12 times lower compared to that of ACh in rat and
285 chicken α9α10 recombinant receptors (~ 10 μM) (Elgoyhen *et al.*, 2001, Lipovsek *et al.*,
286 2012). As previously reported (Elgoyhen *et al.*, 2001), the nicotinic agonist DMPP
287 behaved as a very weak partial agonist of rat α9α10 nAChRs (Fig. 1C and Table 1),
288 with a maximal response that was 0.6 ± 0.3 %, (n=6) of that observed with 1 mM ACh
289 (n=6). Surprisingly, the efficacy of DMPP on chicken α9α10 receptors was significantly
290 higher (p=0.004 Mann-Whitney test compared to rat), reaching 32.6 ± 2.9 % of that of
291 ACh with an EC_{50} of 9.8 ± 0.5 μM (n=5; p=0.03 Mann-Whitney test, chick vs rat).
292 Finally, choline behaved as a partial agonist on rat heteromeric α9α10 receptors (Fig.
293 1D and Table 1), with a maximal response that was 37.5 ± 2.5 % of that produced by 1
294 mM ACh and an EC_{50} of 541 ± 62 μM (n=10). As observed for DMPP, the efficacy of
295 choline on chicken α9α10 receptors was higher than that observed for rat receptors
296 (n=6; p=0.0004 Kruskal-Wallis test), reaching a maximum response of 88 ± 6.7 % of
297 the maximum response to 1 mM ACh, thus behaving closely to a full agonist.
298 Additionally, the EC_{50} of 200 ± 16 μM (n=6) for choline in chicken α9α10 receptors
299 was nearly three times lower than that observed for rat receptors (EC_{50}= 541 ± 62
300 (n=10), p=0.0025 Kruskal-Wallis test). In summary, whilst inhibition by nicotine and
301 agonism by carbachol were similar between chicken and rat receptors, choline and
302 DMPP presented higher efficacies for the avian than for the mammalian α9α10
303 heteromeric nAChRs.

304

305 **Choline elicits near-maximal responses in chicken, but not in mouse, hair cells**

306 Choline is naturally present at cholinergic synapses as a degradation product of ACh
307 (Wehrwein *et al.*, 2016) and its effect on nAChRs can have important implications on

308 synaptic function (Albuquerque *et al.*, 1998). The synapse between efferent fibers and
309 hair cells is mediated by α9α10 nicotinic receptors coupled to the activation of SK2
310 calcium dependent potassium channels, resulting in an inhibitory response (Fuchs &
311 Murrow, 1992, Dulon & Lenoir, 1996, Katz *et al.*, 2004, Gomez-Casati *et al.*, 2005,
312 Elgoyhen & Katz, 2012). We analyzed the effect of choline in mouse and chicken hair
313 cells in acute explants, in comparison to ACh responses. Figure 2A shows
314 representative responses to both ACh and choline at a holding potential of -40 mV.
315 These responses were outward, resulting from the activation of SK2 potassium channels
316 coupled to the cholinergic responses. For both chicken and mouse hair cells we
317 observed maximal responses to 3 mM ACh. However, and in agreement with that
318 observed for recombinant α9α10 receptors, choline exhibited higher efficacy in chicken
319 hair cells (89.7 ± 6.0 %, n=3) when compared to that on mouse hair cells (49.6 ± 8.7 %,
320 n=6; p=0.024 Mann-Whitney test). These observations suggest that the differences in
321 agonistic behavior identified in recombinant α9α10 receptors are recapitulated by the
322 native receptors present in chicken and mouse hair cells.

323

324 **The rat α10 subunit determines choline potency and efficacy in α9α10 nAChRs**

325 In order to determine if the agonistic characteristics of choline could be traced back to
326 the constituent subunits of the α9α10 heteromeric receptors, we first tested the potency
327 of choline on homomeric α9 or α10 nAChRs. Of note, mammalian α10 receptors do not
328 assemble into functional homomeric receptors (Elgoyhen *et al.*, 2001, Sgard *et al.*,
329 2002) and were therefore not tested.

330 Different to that observed for rat heteromeric α9α10 receptors (Fig. 1D), choline
331 behaved as a nearly full agonist of rat α9 receptors (Fig. 3A and Table 1). Thus,
332 although less potent than ACh (EC_{50} choline 188 ± 40, n=3; ACh 12.9 ± 1.1, n=5;
333 p=0.04 Mann-Whitney test), the maximal choline response was 87.3 ± 6.0 % (n=4,
334 p=0.002 Kruskal-Wallis test) compared to that elicited by 1 mM ACh. Additionally, the
335 EC_{50} for choline observed for the rat α9 receptor was smaller than that of the rat α9α10
336 receptor (Fig 1D, 541 ± 62, p=0.02 Kruskal-Wallis test). It is worth noting that on a
337 previous paper we show that choline is nearly a full agonist of rat α9 homomeric
338 receptors, albeit with a higher potency than that observed here (Verbitsky *et al.*, 2000).
339 Differences might derive from the fact that experiments in the present work were
340 performed in the presence of BAPTA-AM to isolate the cholinergic responses from the

341 secondary activation of the Ca^{2+} sensitive chloride current present in oocytes (Miledi &
342 Parker, 1984), whilst this was not the case in our previous work (Verbitsky *et al.*, 2000).

343 Choline had high efficacy in both chicken α9 and α10 homomeric receptors, similar to
344 that observed for the chicken α9α10 heteromeric receptor (Table 1). The maximal
345 choline response in chicken α9 receptors was 73.7 ± 5.9 % (n=6) of that obtained for 1
346 mM ACh (Fig. 3B), and it matched the maximal ACh response, 99.4 ± 9.5 % (n=4), in
347 chicken α10 receptors (Fig. 3C). Choline potency was lower compared to that of ACh
348 for both chicken homomeric receptors and concentration-response curves to choline
349 were shifted to the right with higher EC_{50} values (Fig. 3B-C). For chicken α9, choline
350 showed an EC_{50} = 280 ± 20 μM (n=6) compared to 12.9 ± 1.4 μM for ACh (n=5,
351 p=0.004 Mann-Whitney test). In chicken α10 receptors the EC_{50} for choline was 23.2 ±
352 8.3 μM (n=4), compared to 2.2 ± 0.7 μM for ACh (n=5, p=0.016 Mann-Whitney test).

353 In summary, choline behaved as an agonist with high efficacy in homomeric receptors
354 composed of rat α9, chicken α9 or chicken α10 subunits. This agonistic behavior was
355 similar to that observed for chicken α9α10 receptors but differed from that of rat α9α10
356 heteromeric receptors.

357 The observation that choline behaved as a partial agonist of heteromeric rat α9α10
358 receptors, but a full agonist of rat α9 homomeric nAChRs, suggests that the rat α10
359 subunit may contain determinants responsible for the lower efficacy of choline on
360 heteromeric α9α10 receptors. In order to test this hypothesis, we expressed rat-chicken
361 hybrid receptors in *X. laevis* oocytes (Fig. 4). We previously determined that responses
362 in these hybrid α9α10 receptors are indeed the result of heteromeric assemblies and not
363 individual homomeric receptors (Lipovsek *et al.*, 2014). As shown in Figure 4A, rat α9
364 – chicken α10 hybrid receptors responded to ACh with an EC_{50} of 11.6 ± 2.9 μM (n=7),
365 similar to that of rat (EC_{50} 17.1 ± 3.1 μM, n=5, p=0.19 Kruskal-Wallis test) and chicken
366 (EC_{50} 13.1 ± 2.6 μM, n=10, p=0.67 Kruskal-Wallis test) α9α10 nAChRs (Table 1).
367 Different to that described for rat α9α10 receptors (Fig. 1D), choline produced near
368 maximal responses in rat α9 – chicken α10 hybrid receptors (86.4 ± 2.1 % of responses
369 to 1 mM ACh, n=6), that were similar to those observed in chicken α9α10 receptors (88
370 ± 6.7 %, n = 6). On the other hand, hybrid chicken α9 – rat α10 receptors exhibited
371 similar concentration-response curves to ACh when compared to rat and chicken α9α10
372 receptors, with an EC_{50} of 18.2 ± 4.8 μM (n=4, p=0.99 and p=0.29, respectively,
373 Kruskal-Wallis test; Fig. 4B and Table 1). However, the maximal response to choline of

374 chicken α9 – rat α10 hybrid receptors (51.2 ± 6.0 %, n=5) was smaller than that
375 observed for chicken α9α10 receptors (88 ± 6.7 %, n=10, p=0.02 Kruskal-Wallis test;
376 Fig. 1C), with a lower efficacy, similar to that of rat α9α10 receptors (37.5 ± 2.5 %,
377 n=9, p=0.50 Kruskal-Wallis test).

378 In summary, both the potency and efficacy of choline on rat heteromeric α9α10
379 receptors were lower when compared to all other receptors tested, with the only
380 exception of heteromeric hybrid receptors containing rat α10 subunits, therefore
381 suggesting that the rat α10 subunit may hold the molecular determinants of choline's
382 partial agonism (Fig. 4C).

383

384 **Lower frequency of choline binding at orthosteric sites holding rat α10 subunits as**
385 **complementary component**

386 To gain further insight into the mechanism underlying the drop in choline agonism on
387 receptors containing the rat α10 subunit, we performed molecular docking simulations
388 and analyzed the interaction of ACh and choline with the orthosteric binding site. To
389 this end, we used homology models of the extracellular domains of rat and chicken
390 α9α10 receptors with subunit arrangements corresponding to the four possible binding
391 site interfaces (principal/complementary components): α9/α9, α9/α10, α10/α9 and
392 α10/α10 as previously reported in (Boffi *et al.*, 2017). We then performed molecular
393 docking analysis of the interaction of ACh or choline with the homology-modelled
394 subunit interfaces to evaluate the orientation, the best binding energy (BBE) and the
395 frequency of conformations that bind the agonist in a favorable orientation within the
396 binding pocket. The conformations considered as favorable were those that showed
397 typical cation-π interactions between the amino group of the ligands and aromatic
398 residues of the binding pocket (W55, from the complementary face, and Y93, W149,
399 Y190 and/or Y197 from the principal face) required for ACh responses (Dougherty,
400 2007, Olsen *et al.*, 2014).

401 As reported previously (Boffi *et al.*, 2017), both for rat and chicken receptors, ACh
402 docking resulted in an energetically favorable model with ACh oriented with its
403 quaternary amine toward the membrane side or lower part of the cleft and the negative
404 charge oriented upwards in the cleft (Fig. 5A and B), similarly to ACh in AChBP
405 (Olsen *et al.*, 2014). In this orientation, ACh showed BBE between -3.5 and -6 kcal/mol

406 for the different binding interfaces (Fig. 5E) and its positively charged group showed
407 the potential to form the typical cation-π interactions with the main aromatic residues
408 Y93, W149, Y190, Y197 and W55 (Fig. 5B and C). Thus, as reported for other
409 nAChRs, the orientation of ACh in the binding pocket of rat and chicken α9α10
410 receptors is favorable for efficacious activation (Fig. 5 and (Boffi *et al.*, 2017)).

411 For all interfaces, choline docked into the orthosteric binding site with two different
412 orientations. The least frequent orientation was similar to that described for choline
413 docked into the muscle nAChR (Bruhova & Auerbach, 2017). In the most frequent and
414 lowest BBE conformation, choline was located more horizontal with respect to the
415 membrane compared to ACh, oriented towards the C-loop containing Y190 and Y197,
416 with the quaternary ammonium placed in the aromatic cavity (Fig. 5B and D). This
417 orientation has also been described for other ligands in different nAChR models
418 (Tomaselli *et al.*, 1991, Lester *et al.*, 2004, Hernando *et al.*, 2012). In this orientation,
419 choline showed the potential to make typical cation-π interactions with the aromatic
420 residues at the principal (W149, Y190, Y197, but not Y93) and complementary (W55)
421 components (Fig. 5D). Whereas ACh formed an H-bond with the backbone amine
422 group of residue D119 (Boffi, 2017 and Fig. 5B and C), choline formed an H-bond with
423 the carboxyl group of D119 (Fig. 5B and D). Altogether, the orientation and potential
424 interactions with residues indicate that choline adopts a favorable conformation (though
425 different to that of ACh) for eliciting receptor activation, with lower BBEs than those
426 observed for ACh (between -4 and -4.5 kcal/ mol for all interfaces).

427 The orientation and main interactions of choline with residues at the binding site were
428 identical for all interfaces and between chicken and rat receptors. Also, while the BBE
429 for choline did not show significant inter-species differences across the different
430 interfaces, we observed differences in the frequency at which choline bound with
431 favorable conformations to the different interfaces (Fig. 5E). Those binding interfaces
432 containing α9 as the complementary subunit (α9/α9 and α10/α9) showed higher
433 frequency of choline binding in the favorable conformations but did not show
434 differences between chicken and rat subunits (Fig. 5E). In contrast, differences were
435 encountered at interfaces in which α10 provided the complementary side (α9/α10 and
436 α10/α10). Whilst each agonist binding frequency for chicken interfaces was similar to
437 that observed when α9 acts as the complementary subunit, it was significantly lower for
438 interfaces showing a rat α10 complementary subunit (Fig. 5F).

439 Thus, our *in silico* studies focused on the binding site interfaces suggest that the
440 differences of choline responses may be governed by the distinct choline orientation and
441 the differential contribution of binding interfaces containing α10 as the complementary
442 subunit. Whilst in chicken α9α10 receptors a high frequency of choline binding was
443 observed for all conformations of binding sites, in rat α9α10 receptors the frequency of
444 choline binding was significantly lower at α9/α10 and α10/α10 sites, suggesting that the
445 lower choline agonism observed in rat α10 containing receptors (Figures 3 and 4) may
446 be related to a reduced capability of the rat α10 subunit to efficiently operate as the
447 complementary side during agonist binding and receptor gating. Consequently, a
448 reduction in the binding frequency of agonists at specific interfaces might determine
449 alternate responses in the context of receptor function.

450

451 **The extracellular region of the rat α10 subunit underpins lower choline efficacy**

452 The N-terminal and TM2-TM3 extracellular domains of nicotinic receptors bare
453 residues involved both in agonist binding and coupling to pore opening (Karlin, 2002,
454 Bouzat *et al.*, 2004), and most likely contain determinants for agonist efficacy (Gupta *et*
455 *al.*, 2017, Mukhtasimova & Sine, 2018). Given that choline partial agonism is observed
456 when rat α10 subunits are present in the heteromeric receptors (Fig. 4C) and that,
457 although it binds to all binding site combinations, the frequency of favorable choline
458 binding was lower at interfaces in which rat α10 provided the complementary face (Fig.
459 5F), we hypothesized that a receptor in which no binding site contains α10 components
460 would show strong choline agonism. To test this, we engineered a rat α9-α10 ($\alpha10_x$)
461 chimeric subunit in which the entire N-terminal and TM2-TM3 extracellular regions of
462 the rat α10 subunit were replaced by the corresponding domains of the rat α9 subunit
463 (Fig. 6A). The chimeric subunit did not form functional homomeric receptors by itself,
464 nor did it do so when co-expressed with the rat α10 subunit. However, when co-
465 expressed with the rat α9 subunit, strong ACh responses were recorded for rat $\alpha9\alpha10_x$
466 receptors (Fig. 6B), with I_{max} = 269.0 ± 103.1 nA (n=5). This contrasts the maximal
467 ACh responses observed for homomeric rat α9 receptors (I_{max} of 13.8 ± 2.1 nA, n=4 and
468 see (Elgoyhen *et al.*, 2001), indicating that, when co-expressed, rat α9 and chimeric
469 $\alpha10_x$ subunits form heteromeric assemblies. Concentration-response curves to ACh of
470 rat $\alpha9\alpha10_x$ receptors were similar to those of rat α9α10 wild-type receptors with an EC_{50}
471 of 15.6 ± 6.5 μM (n=4, p=0.50 Kruskal-Wallis test) (Fig. 6C). Interestingly, responses

472 to choline of the rat α9α10$_x$ chimeric receptor resembled those exhibited by rat α9
473 homomeric receptors and differed from those rat α9α10 receptors. Thus, the EC_{50} for
474 choline on α9α10$_x$ receptors was 160.2 ± 7.6 μM (n=5), significantly smaller than that
475 in rat α9α10 receptors (541 ± 62 μM, n=10, p=0.007, Kruskal-Wallis test) and similar to
476 that observed in homomeric rat α9 receptors (Fig. 6C and Table 1). Likewise, choline
477 evoked maximal response of 74.3 ± 1.0% (n=5) in α9α10$_x$ receptors was higher than
478 that of rat α9α10 (37.5 ± 2.5 %, n=9, p=0.04 Kruskal-Wallis test) but similar to that
479 observed in rat α9 homomeric receptors (87.3 ± 6.0 %, n=4, p=0.27, Kruskal-Wallis
480 test) (Fig. 6C and Table 1). Taken together, the experimental evaluation of ACh and
481 choline agonism in a chimeric receptor indicates that the extracellular region of the rat
482 α10 subunit bears determinants that render an α9α10 receptor on which choline has low
483 efficacy.

484

485 **The α10 complementary component participates in activation by choline of rat**
486 **α9α10 nAChRs**

487 In a previous work we showed that rat α10 subunits do not contribute with
488 complementary faces to the ACh binding site (Boffi *et al.*, 2017). In contrast, in the
489 present study we have so far shown that the extracellular domain of the rat α10 subunit
490 is responsible for the decrease in choline agonism in rat α9α10 receptors. Moreover, *in*
491 *silico* docking showed that the frequency of choline binding in the correct conformation
492 is lower at interfaces where the complementary component is provided by rat α10
493 subunits (Fig. 5E), suggesting that the lower choline agonism observed in rat α9α10
494 receptors may result from sub-functional α9/α10 or α10/α10 binding sites. Therefore, to
495 experimentally evaluate choline's requirement for functional binding sites containing
496 α10 complementary components, we studied responses to choline on rat α9α10
497 heteromeric receptors holding the W55T mutation in the rat α10 subunits (Fig. 7A).
498 While responses to ACh showed no significant changes in the α9α10W55T receptor
499 compared to wild type α9α10 receptors (Boffi *et al.*, 2017), Fig. 7A and B and Table 1 -
500 EC_{50} α9α10: 17.1 ± 3.1 μM, n=5; EC_{50} α9α10W55T: 37.8 ± 6.2 μM, n=8; p=0.06,
501 Kruskal-Wallis test), responses to choline were nearly abolished in mutant receptors on
502 which responses to 10 mM choline were 7.4 ± 1.9 % (n=5) of those elicited by 1 mM
503 ACh (Fig. 7B). This indicates that the contribution of the complementary face of the rat
504 α10 subunit to the agonistic effect of ACh and choline is non-equivalent. Thus, whereas

505 rat α10 complementary faces are not required for ACh activation of rat α9α10 receptors
506 (see also (Boffi *et al.*, 2017), intact rat α10 complementary components are required for
507 choline agonistic effect.

508 Finally, to evaluate whether choline interacts with the α10/α9 intact interfaces in the
509 α9α10W55T receptor, and therefore also requires them to elicit its reduced agonism, we
510 analyzed responses to 10 μM ACh in the presence of increasing concentrations of
511 choline for both rat α9α10 and α9α10W55T receptors (Fig. 7C and D). ACh was added
512 once a maximal response to choline was observed. The maximal response obtained
513 during the co-application was normalized to the response to 10 μM ACh (Fig. 7C). At
514 low choline concentrations that do not trigger channel opening (< 100 μM), ACh
515 responses became increasingly smaller as choline concentration increased, both in the
516 α9α10 and the α9α10W55T receptors, suggesting that choline is capable of competing
517 with ACh for the available binding sites. However, in the presence of higher choline
518 concentrations (>300 μM), total responses in α9α10 receptors increased while they
519 remained unchanged for the mutant receptor (Fig. 7D). The V-shaped effect observed in
520 the α9α10 receptor, where an EC_{50} ACh response is blocked at low concentrations of
521 choline and summation of both agonist responses occurs at higher choline
522 concentrations, is consistent with choline acting as a partial agonist (Zhu, 2005) and
523 suggests that the increase in combined response may be due to choline binding to the
524 α9/α10 and α10/α10 sites that are spared by ACh. Conversely, the lack of increase of
525 ACh responses at higher choline concentrations in the α9α10W55T mutant receptor
526 indicates a loss of choline agonism that may result from the unavailability of additional
527 α9/α10 and α10/α10 sites due to the W55T mutation.

528 Overall, the differences observed in the responses to ACh and/or choline between
529 α9α10 wild type and α9α10W55T mutant receptors indicate that the complementary
530 faces of α10 subunits are required for the partial agonistic effect of choline on α9α10
531 receptors, therefore suggesting that choline necessitates higher binding site occupancy
532 compared to ACh to elicit channel gating of rat α9α10 nAChRs.

533

534 **Discussion**

535 The present work shows that the mammalian (rat) α10 nAChR subunit is responsible for
536 a reduced efficacy of choline when assembled into heteromeric α9α10 receptors. Thus,

537 whereas choline is a full agonist of rat α9 homomeric receptors, it is a partial agonist of
538 rat α9α10 nAChRs. This is further supported by hybrid receptors, on which choline is a
539 full agonist of rat α9 – chicken α10 receptors and the efficacy in chicken heteromeric
540 receptors is reduced when the chicken α10 subunit is replaced by the rat α10 subunit in
541 the chicken α9 – rat α10 assembly. The reduced agonist efficacy determined by the rat
542 α10 subunit is probably extended to other compounds that behave as partial agonists, as
543 evidenced in the present work for DMPP. These results add to the differential functional
544 properties between mammalian and non-mammalian vertebrate α9α10 nAChRs, that
545 have been shaped by the more prevalent occurrence of non-synonymous amino acid
546 substitutions during the evolution of mammalian subunits (Franchini & Elgoyhen, 2006,
547 Elgoyhen & Franchini, 2011, Lipovsek *et al.*, 2012, Lipovsek *et al.*, 2014, Marcovich *et*
548 *al.*, 2020).

549 Full and partial agonists evoke distinct structural changes in opening the muscle
550 acetylcholine receptor channel (Mukhtasimova & Sine, 2018). This is further supported
551 by the observation that the αE45R mutation within the binding–gating transduction
552 domain of this receptor attenuates channel opening by a full agonist, whereas it
553 enhances channel opening by a partial agonist (Mukhtasimova & Sine, 2013). It was
554 therefore suggested that, due to differences in size and/or chemical structure, different
555 agonists of the same receptor might bind in different conformations and/or strength to
556 the ligand interaction pocket (Mukhtasimova & Sine, 2018). This resembles our
557 observations on the effect of mutating W55, a residue located within loop D of the
558 complementary component of the binding site, which by directly interacting with the
559 agonist is crucial for binding-gating transduction (Olsen *et al.*, 2014). In the present
560 work, the W55T mutation in the rat α10 subunit greatly impairs the response of the
561 α9α10 receptor to choline but not to ACh.

562 This functional non-equivalence is further supported by docking analysis, which shows
563 that ACh and choline adopt different conformations at the binding site of α9α10
564 receptors. This result fully agrees with previous studies in the muscle nAChR (Bruhova
565 & Auerbach, 2017), for which choline and ACh sit at different orientations at the
566 binding site. In our model, choline had two probable alternate orientations compared to
567 ACh with the least frequent one resembling the one described for the muscle nAChR
568 (Bruhova & Auerbach, 2017). Furthermore, the non-equivalence of the agonist binding
569 sites for ACh and choline is reflected in differential atomic interactions. Thus, similar to

570 ACh, choline can make interactions at the aromatic cage. However, whereas ACh
571 makes a H-bond with the backbone amine group of D119 of the complementary face,
572 choline shows the potential to make a H-bond with the carboxyl group of the same
573 residue (Fig. 5B and D). Similar to that reported for the muscle ACh receptor (Bruhova
574 & Auerbach, 2017), this different orientation leads to the displacement of the quaternary
575 ammonium of choline away from a favorable position in the aromatic cage compared to
576 ACh. This might lead to a weaker interaction with all aromatic rings of the binding site,
577 accounting for the lower apparent affinity of choline compared to ACh for the α9α10
578 receptor. Moreover, due to the particular orientation of choline towards the C-loop when
579 compared to ACh, differential interactions with residues of the complementary face
580 and/or degree of closure of the C-loop required for channel gating (Thompson *et al.*,
581 2010), might be involved in the reduced choline efficacy.

582 Our combined *in silico* and experimental observations allow us further insight into the
583 differential responses to ACh and choline of rat α9α10 nAChRs. Whereas the
584 complementary face of the α10 subunit does not play an important role in the activation
585 of the receptor by ACh, it is strictly required for choline responses, as shown by the
586 results of the W55T mutation. ACh adopts a different and more favorable conformation,
587 better placed withing the aromatic pocket compared to choline, and would therefore
588 only require occupying two of the five binding sites, sparing binding sites in which the
589 complementary face is provided by the α10 subunit. However, since choline adopts a
590 less favorable conformation, it probably requires higher binding site occupancy for full
591 efficacy. Differences in agonist efficacy according to available binding sites have been
592 reported for other nAChRs. For example, the α4β2 nAChR in the $(\alpha4)_3(\beta2)_2$
593 stoichiometry contains three functional agonist binding sites for ACh (Harpsøe *et al.*,
594 2011, Mazzaferro *et al.*, 2011), and the engagement of all three agonist sites produces
595 maximal activation. The agonist site at the α4/α4 interface is a key determinant of
596 agonist efficacy as occupancy of this site increases agonist efficacy, whereas exclusion
597 from the site leads to partial agonism (Mazzaferro *et al.*, 2014). Another example is
598 provided by the α7 receptor. Even though maximal activation requires occupancy of
599 three binding sites in the α7-5hT3A chimera (Rayes *et al.*, 2009), only one is required in
600 the α7 nAChR (Andersen *et al.*, 2013). Thus, the relationship between binding site
601 occupancy and maximal response differs between nAChRs. Moreover, and in light of

602 our results, we propose that the degree of occupancy required for maximal responses
603 varies with the type of agonist.

604 Hair cell α9α10 nAChRs are distinct from other nicotinic receptors in that a greater
605 divergence in their coding sequence has translated into differential functional properties
606 across clades (Lipovsek *et al.*, 2012, Lipovsek *et al.*, 2014, Marcovich *et al.*, 2020). Our
607 observations here that choline, the degradation product of ACh, has differential
608 agonistic effects on rodent vs avian α9α10 receptors, suggests different scenarios for the
609 workings of the respective efferent synapsis. Recordings on native cholinergic
610 responses recapitulated our observations in recombinant rat and chick α9α10 receptors.
611 While choline elicited maximal responses in chicken hair cells, it behaved as a partial
612 agonist of the native nicotinic receptors present in hair cells of mice (Fig. 2). In chicken
613 efferent synapsis to (mostly) short hair cells, the release of ACh from efferent terminals
614 triggers α9α10 receptors that would continue to be activated in response to the choline
615 produced by ACh degradation due to acetylcholinesterase (AChE) activity, until it is
616 removed from the synaptic cleft. This would result in longer post-synaptic responses
617 subjected to large variations and poor temporal tuning (Katz & Miledi, 1973). In
618 contrast, in mammalian efferent olivocochlear synapses, the degradation of ACh to
619 choline would limit the time-course and improve the reliability of the cholinergic
620 response. Given that choline is not able to fully activate the rodent α9α10 receptor, and
621 in the presence of ACh acts as a competitive antagonist, the termination of α9α10
622 responses would therefore be dictated by the fast kinetics of AChE activity (Hall, 1973).
623 An apical to basal concentration and isoform diversity gradient of AChE has been
624 described in the mouse cochlea (Emmerling & Sobkowicz, 1988). Notably, the high-
625 frequency basal region exhibits higher concentrations of this enzyme and is enriched in
626 isoforms with faster kinetics, underscoring the relevance of fine temporal tunning of
627 efferent modulation for high frequency sound detection (Emmerling & Sobkowicz,
628 1988). Also, compared to chicken, the mammalian α9α10 receptor shows greater
629 desensitization to ACh and higher calcium permeability that may result in uncoupling
630 from internal calcium stores (Lipovsek *et al.*, 2012, Lipovsek *et al.*, 2014, Marcovich *et*
631 *al.*, 2020). Together with the poorer choline agonism, these functional adaptations that
632 lead to "tighter" ACh responses, may prove fundamental for the high-frequency
633 modulation of the prestin-driven amplifier of mammalian outer hair cells, by allowing

634 post-synaptic summation to faithfully reproduce high frequency activity of efferent
635 medial olivocochlear fibers (Ballestero *et al.*, 2011).

636 The lower agonistic action of choline on mammalian α9α10 receptors is likely due to
637 the accumulation of amino acid changes within the mammalian α10 subunit (Franchini
638 & Elgoyhen, 2006, Lipovsek *et al.*, 2012) that rendered a subfunctional contribution of
639 α10 as a complementary component subunit. Our *in silico* and experimental analysis of
640 choline agonism indicate that, for it to trigger a full response, it needs to bind to α9/α10
641 and/or α10/α10 sites, therefore requiring sites holding α10 complementary interfaces.
642 This is in contrast with the agonism by ACh, that only requires binding to α10/α9 (or
643 α9/α9) sites formed by an α10 (or α9) principal component and α9 complementary
644 component (Boffi *et al.*, 2017). We hypothesize that amino acid changes within the α10
645 subunit that affect agonist binding and/or receptor triggering from the additional binding
646 sites (i.e. those that have an α10 subunit as a complementary component) would not be
647 deleterious and therefore not under negative selection, as they would not affect the main
648 response to ACh, given that the sensitivity for this agonist is the same in the different
649 species (Lipovsek *et al.*, 2012, Marcovich *et al.*, 2020).

650 In this context, a scenario could be proposed in which strong positive selection pressure
651 for the loss of the agonistic function of choline, a likely functional requirement for fine-
652 tuned high-frequency efferent olivocochlear activity, may have been the driver for the
653 accumulation of coding sequence changes within the extracellular domain of
654 mammalian α10 subunits (Franchini & Elgoyhen, 2006). This then resulted in the loss
655 of choline acting as a full agonism for mammalian α9α10 receptors, without affecting
656 the triggering of ACh responses.

657

658 **References**

659 Albuquerque EX, Pereira EF, Braga MF & Alkondon M (1998) Contribution of
660 nicotinic receptors to the function of synapses in the central nervous system: the action
661 of choline as a selective agonist of alpha 7 receptors. *J Physiol Paris* **92**: 309-316.

662 Andersen N, Corradi J, Sine SM & Bouzat C (2013) Stoichiometry for activation of
663 neuronal α7 nicotinic receptors. *Proc Natl Acad Sci U S A* **110**: 20819-20824.

664 Arnold K, Bordoli L, Kopp J & Schwede T (2006) The SWISS-MODEL workspace: a
665 web-based environment for protein structure homology modelling. *Bioinformatics* **22**:
666 195-201.

667 Ballestero J, Zorrilla de San Martin J, Goutman J, Elgoyhen AB, Fuchs PA & Katz E
668 (2011) Short-term synaptic plasticity regulates the level of olivocochlear inhibition to
669 auditory hair cells. *J Neurosci* **31**: 14763-14774.

670 Boffi JC, Marcovich I, Gill-Thind JK*, et al.* (2017) Differential Contribution of Subunit
671 Interfaces to alpha9alpha10 Nicotinic Acetylcholine Receptor Function. *Molecular*
672 *pharmacology* **91**: 250-262.

673 Bordoli L, Kiefer F, Arnold K, Benkert P, Battey J & Schwede T (2009) Protein
674 structure homology modeling using SWISS-MODEL workspace. *Nature protocols* **4**: 1-
675 13.

676 Bouzat C, Gumilar F, Spitzmaul G, Wang HL, Rayes D, Hansen SB, Taylor P & Sine
677 SM (2004) Coupling of agonist binding to channel gating in an ACh-binding protein
678 linked to an ion channel. *Nature* **430**: 896-900.

679 Bruhova I & Auerbach A (2017) Molecular recognition at cholinergic synapses:
680 acetylcholine versus choline. *J Physiol* **595**: 1253-1261.

681 Dougherty DA (2007) Cation-pi interactions involving aromatic amino acids. *The*
682 *Journal of nutrition* **137**: 1504S-1508S; discussion 1516S-1517S.

683 Dulon D & Lenoir M (1996) Cholinergic responses in developing outer hair cells of the
684 rat cochlea. *European J Neurosci* **8**: 1945-1952.

685 Elgoyhen AB & Franchini LF (2011) Prestin and the cholinergic receptor of hair cells:
686 Positively-selected proteins in mammals. *Hear Res* **273**: 100-108.

687 Elgoyhen AB & Katz E (2012) The efferent medial olivocochlear-hair cell synapse. *J*
688 *Physiol Paris* **106**: 47-56.

689 Elgoyhen AB, Katz E & Fuchs PA (2009) The nicotinic receptor of cochlear hair cells:
690 a possible pharmacotherapeutic target? *Biochemical pharmacology* **78**: 712-719.

691 Elgoyhen AB, Johnson DS, Boulter J, Vetter DE & Heinemann S (1994) a9: an
692 acetylcholine receptor with novel pharmacological properties expressed in rat cochlear
693 hair cells. *Cell* **79**: 705-715.

694 Elgoyhen AB, Vetter D, Katz E, Rothlin C, Heinemann S & Boulter J (2001) Alpha 10:
695 A determinant of nicotinic cholinergic receptor function in mammalian vestibular and
696 cochlear mechanosensory hair cells. *Proc Natl Acad Sci USA* **98**: 3501-3506.

697 Emmerling MR & Sobkowicz HM (1988) Differentiation and distribution of
698 acetylcholinesterase molecular forms in the mouse cochlea. *Hear Res* **32**: 137-145.

699 Franchini LF & Elgoyhen AB (2006) Adaptive evolution in mammalian proteins
700 involved in cochlear outer hair cell electromotility. *Mol Phylogenet Evol* **41**: 622-635.

701 Fuchs PA & Murrow BW (1992) A novel cholinergic receptor mediates inhibition of
702 chick cochlear hair cells. *Proc R Soc Lond B* **248**: 35-40.

703 Gomez-Casati ME, Fuchs PA, Elgoyhen AB & Katz E (2005) Biophysical and
704 pharmacological characterization of nicotinic cholinergic receptors in cochlear inner
705 hair cells. *J Physiol* **566**: 103-118.

706 Goutman JD, Elgoyhen AB & Gomez-Casati ME (2015) Cochlear hair cells: The
707 sound-sensing machines. *FEBS Lett* **589**: 3354-3361.

708 Guex N & Peitsch MC (1997) SWISS-MODEL and the Swiss-PdbViewer: an
709 environment for comparative protein modeling. *Electrophoresis* **18**: 2714-2723.

710 Gupta S, Chakraborty S, Vij R & Auerbach A (2017) A mechanism for acetylcholine
711 receptor gating based on structure, coupling, phi, and flip. *The Journal of general*
712 *physiology* **149**: 85-103.

713 Hall ZW (1973) Multiple forms of acetylcholinesterase and their distribution in endplate
714 and non-endplate regions of rat diaphragm muscle. *Journal of neurobiology* **4**: 343-361.

715 Harpsøe K, Ahring PK, Christensen JK, Jensen ML, Peters D & Balle T (2011)
716 Unraveling the high- and low-sensitivity agonist responses of nicotinic acetylcholine
717 receptors. *J Neurosci* **31**: 10759-10766.

718 Hernando G, Bergé I, Rayes D & Bouzat C (2012) Contribution of subunits to
719 Caenorhabditis elegans levamisole-sensitive nicotinic receptor function. *Molecular*
720 *pharmacology* **82**: 550-560.

721 Horton RM, Hunt HD, Ho SN, Pullen JK & Pease LR (1989) Engineering hybrid genes
722 without the use of restriction enzymes: gene splicing by overlap extension. *Gene (Amst)*
723 **77**: 61-68.

724 Humphrey W, Dalke A & Schulten K (1996) VMD: visual molecular dynamics.
725 *Journal of molecular graphics* **14**: 33-38, 27-38.

726 Karlin A (2002) Ion channel structure: emerging structure of the nicotinic acetylcholine
727 receptors. *Nature Reviews Neurosc* **3**: 102-114.

728 Katz B & Miledi R (1973) The binding of acetylcholine to receptors and its removal
729 from the synaptic cleft. *J Physiol* **231**: 549-574.

730 Katz E & Elgoyhen AB (2014) Short-term plasticity and modulation of synaptic
731 transmission at mammalian inhibitory cholinergic olivocochlear synapses. *Front Syst*
732 *Neurosci* **8**: 224.

733 Katz E, Elgoyhen AB, Gomez-Casati ME, Knipper M, Vetter DE, Fuchs PA &
734 Glowatzki E (2004) Developmental regulation of nicotinic synapses on cochlear inner
735 hair cells. *J Neurosci* **24**: 7814-7820.

736 Lester HA, Dibas MI, Dahan DS, Leite JF & Dougherty DA (2004) Cys-loop receptors:
737 new twists and turns. *Trends Neurosci* **27**: 329-336.

738 Lipovsek M, Im GJ, Franchini LF, Pisciottano F, Katz E, Fuchs PA & Elgoyhen AB
739 (2012) Phylogenetic differences in calcium permeability of the auditory hair cell
740 cholinergic nicotinic receptor. *Proc Natl Acad Sci U S A* **109**: 4308-4313.

741 Lipovsek M, Fierro A, Perez EG, Boffi JC, Millar NS, Fuchs PA, Katz E & Elgoyhen
742 AB (2014) Tracking the molecular evolution of calcium permeability in a nicotinic
743 acetylcholine receptor. *Mol Biol Evol* **31**: 3250-3265.

744 Manley GA (2000) Cochlear mechanisms from a phylogenetic viewpoint. *Proc Natl*
745 *Acad Sci U S A* **97**: 11736-11743.

746 Marcovich I, Moglie MJ, Carpaneto Freixas AE, Trigila AP, Franchini LF, Plazas PV,
747 Lipovsek M & Elgoyhen AB (2020) Distinct Evolutionary Trajectories of Neuronal and
748 Hair Cell Nicotinic Acetylcholine Receptors. *Mol Biol Evol* **37**: 1070-1089.

749 Mazzaferro S, Benallegue N, Carbone A, Gasparri F, Vijayan R, Biggin PC, Moroni M
750 & Bermudez I (2011) Additional acetylcholine (ACh) binding site at alpha4/alpha4
751 interface of (alpha4beta2)2alpha4 nicotinic receptor influences agonist sensitivity. *The*
752 *Journal of biological chemistry* **286**: 31043-31054.

753 Mazzaferro S, Gasparri F, New K, Alcaino C, Faundez M, Iturriaga Vasquez P, Vijayan
754 R, Biggin PC & Bermudez I (2014) Non-equivalent ligand selectivity of agonist sites in
755 (α4β2)2α4 nicotinic acetylcholine receptors: a key determinant of agonist efficacy. *The*
756 *Journal of biological chemistry* **289**: 21795-21806.

757 Miledi R & Parker I (1984) Chloride current induced by injection of calcium into
758 Xenopus oocytes. *J Physiol (Lond)* **357**: 173-183.

759 Morris GM, Huey R, Lindstrom W, Sanner MF, Belew RK, Goodsell DS & Olson AJ
760 (2009) AutoDock4 and AutoDockTools4: Automated docking with selective receptor
761 flexibility. *J Comput Chem* **30**: 2785-2791.

762 Mukhtasimova N & Sine SM (2013) Nicotinic receptor transduction zone: invariant
763 arginine couples to multiple electron-rich residues. *Biophysical journal* **104**: 355-367.

764 Mukhtasimova N & Sine SM (2018) Full and partial agonists evoke distinct structural
765 changes in opening the muscle acetylcholine receptor channel. *The Journal of general*
766 *physiology* **150**: 713-729.

767 Olsen JA, Balle T, Gajhede M, Ahring PK & Kastrup JS (2014) Molecular recognition
768 of the neurotransmitter acetylcholine by an acetylcholine binding protein reveals
769 determinants of binding to nicotinic acetylcholine receptors. *PLoS One* **9**: e91232.

770 Pujol R, Lavigne-Revillard M & Lenoir M (1998) Development of Sensory and Neural
771 Structures in the Mammalian Cochlea. *Development of the Auditory System,*(Rubel E,
772 Popper A & Fay R, eds.), p.^pp. 146-192. Springer, New York.

773 Rayes D, De Rosa MJ, Sine SM & Bouzat C (2009) Number and locations of agonist
774 binding sites required to activate homomeric Cys-loop receptors. *J Neurosci* **29**: 6022-
775 6032.

776 Rothlin C, Verbitsky M, Katz E & Elgoyhen A (1999) The α9 nicotinic acetylcholine
777 receptor shares pharmacological properties with type A γ-aminobutyric acid, glycine
778 and type 3 serotonin receptors. *Molec Pharmacol* **55**: 248-254.

779 Rothlin CV, Lioudyno MI, Silbering AF, Plazas PV, Casati ME, Katz E, Guth PS &
780 Elgoyhen AB (2003) Direct interaction of serotonin type 3 receptor ligands with
781 recombinant and native alpha 9 alpha 10-containing nicotinic cholinergic receptors.
782 *Molecular pharmacology* **63**: 1067-1074.

783 Russell RB & Barton GJ (1992) Multiple protein sequence alignment from tertiary
784 structure comparison: assignment of global and residue confidence levels. *Proteins* **14**:
785 309-323.

786 Schwede T, Kopp J, Guex N & Peitsch MC (2003) SWISS-MODEL: An automated
787 protein homology-modeling server. *Nucleic Acids Res* **31**: 3381-3385.

788 Sgard F, Charpentier E, Bertrand S, Walker N, Caput D, Graham D, Bertrand D &
789 Besnard F (2002) A novel human nicotinic receptor subunit, α10, that confers
790 functionality to the α9-subunit. *Molec Pharmacol* **61**: 150-159.

791 Simmons DD (2002) Development of the inner ear efferent system across vertebrate
792 species. *Journal of neurobiology* **53**: 228-250.

793 Thompson AJ, Lester HA & Lummis SC (2010) The structural basis of function in Cys-
794 loop receptors. *Quarterly reviews of biophysics* **43**: 449-499.

795 Tomaselli GF, McLaughlin JT, Jurman ME, Hawrot E & Yellen G (1991) Mutations
796 affecting agonist sensitivity of the nicotinic acetylcholine receptor. *Biophysical journal*
797 **60**: 721-727.

798 Verbitsky M, Rothlin C, Katz E & Elgoyhen AB (2000) Mixed nicotinic-muscarinic
799 properties of the a9 nicotinic cholinergic receptor. *Neuropharmacology* **39**: 2515-2524.

800 Wehrwein EA, Orer HS & Barman SM (2016) Overview of the Anatomy, Physiology,
801 and Pharmacology of the Autonomic Nervous System. *Comprehensive Physiology* **6**:
802 1239-1278.

803 Zhu BT (2005) Mechanistic explanation for the unique pharmacologic properties of
804 receptor partial agonists. *Biomedicine & pharmacotherapy = Biomedecine &*
805 *pharmacotherapie* **59**: 76-89.

806 Zouridakis M, Giastas P, Zarkadas E, Chroni-Tzartou D, Bregestovski P & Tzartos SJ
807 (2014) Crystal structures of free and antagonist-bound states of human α9 nicotinic
808 receptor extracellular domain. *Nature structural & molecular biology* **21**: 976-980.

809

810 **Acknowledgments:**

811 We thank Paul A. Fuchs for assistance in the performance of chicken hair cell
812 recordings. This work was supported by Agencia Nacional de Promoción Científicas y

Técnicas, Argentina, the Scientific Grand Prize of the Fondation Pour l'Audition, and NIH grant R01 DC001508 (Paul Fuchs PI and ABE co-PI) to A.B.E.

816 **Table 1.** Estimated values of EC_{50} and efficacy for agonists of α9α10 receptors and IC_{50}
817 value for the antagonist nicotine. Values are mean ± S.E.M.. Between brackets, number
818 of oocytes per experiment.
819
820

	ACh	Choline		Carbachol		DMPP		Nicotine
	EC_{50} (μM)	EC_{50} (μM)	Efficacy (%)	EC_{50} (μM)	Efficacy (%)	EC_{50} (μM)	Efficacy (%)	IC_{50} (μM)
Rat α9	12.9 ± 1.1 (5)	188 ± 40 (3)	87.3 ± 6.0 (4)	N.D.	N.D.	N.D.	N.D.	N.D.
Rat α9α10	17.1 ± 3.1 (5)	541 ± 62 (10)	37.5 ± 2.5 (9)	159 ± 31.5 (5)	75.5 ± 5.2 (5)	21.5 ± 4.0 (6)	0.6 ± 0.3 (6)	46.3 ± 12.4 (6)
Chicken α9	12.9 ± 1.4 (5)	280 ± 20 (6)	73.7 ± 5.9 (6)	N.D.	N.D.	N.D.	N.D.	N.D.
Chicken α10	2.2 ± 0.7 (5)	23.2 ± 8.3 (4)	99.4 ± 9.5 (4)	N.D.	N.D.	N.D.	N.D.	N.D.
Chicken α9α10	13.1 ± 2.6 (10)	200 ± 16 (6)	88.0 ± 6.7 (6)	150.1 ± 14.8 (6)	89.8 ± 7.0 (6)	9.8 ± 0.5 (5)	32.6 ± 2.9 (5)	39.4 ± 3.4 (6)
Rα9-Cα10	11.6 ± 2.9 (7)	148 ± 12.1 (5)	86.4 ± 2.1 (6)	N.D.	N.D.	N.D.	N.D.	N.D.
Cα9-Rα10	18.2 ± 4.8 (4)	333 ± 66.2 (4)	51.2 ± 6 (5)	N.D.	N.D.	N.D.	N.D.	N.D.
$α9α10_x$	15.6 ± 6.5 (4)	160.2 ± 7.6 (5)	74.3 ± 1.0 (5)	N.D.	N.D.	N.D.	N.D.	N.D.
α9α10W55T	37.8 ± 6.2 (8)	N.D.	7.4 ± 1.9 (5)	N.D.	N.D.	N.D.	N.D.	N.D.

821

823 **Figures**

824 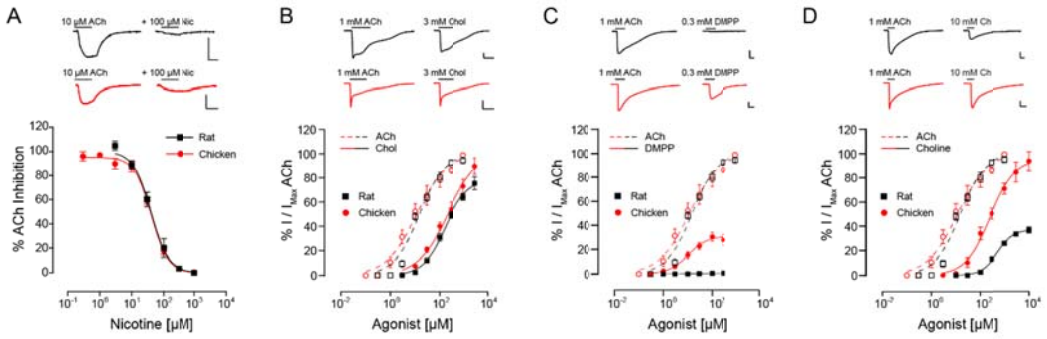

836 **Figure 1.** *Responses of rat and chicken recombinant heteromeric α9α10 nAChRs to*
837 *nicotinic agonists.* A. Upper panels: representative traces of responses to 10 μM ACh
838 (left) blocked by co-application of 100 μM nicotine (right) for rat (black traces) and
839 chicken (red traces) α9α10 receptors. Lower panel: inhibition curves for nicotine for rat
840 and chicken α9α10 receptors. Responses to 10 μM ACh, co-applied with increasing
841 concentrations of nicotine were normalized to the responses to 10 μM ACh alone.
842 Values are mean ± S.E.M. for 6-7 oocytes. B-D. Upper panels: representative maximal
843 responses to ACh (dotted lines) and carbachol (B), DMPP (C) and choline (D) (solid
844 lines) for rat and chicken α9α10 receptors. Lower panels: concentration-response curves
845 for ACh and carbachol (B), DMPP (C) and choline (D) for rat and chicken α9α10
846 receptors. Values are normalized to the maximal response to ACh obtained in each
847 oocyte. Values are mean ± S.E.M. for 5-9 oocytes.

837

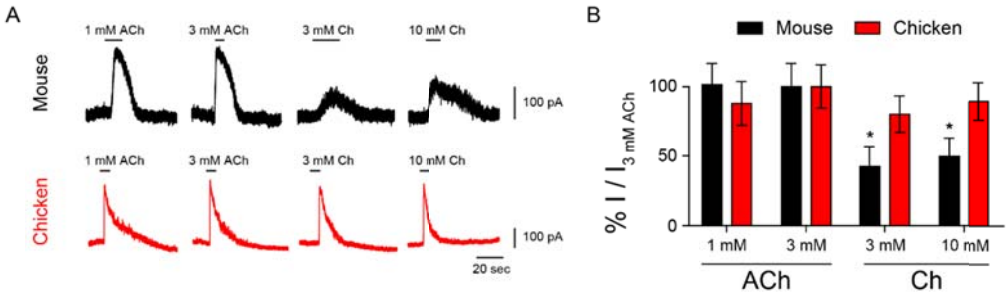

Figure 2. *Responses of hair cells to choline.* **A.** Representative traces of responses to ACh or choline (Ch) in mouse outer (black, upper panel) and chicken short (red, lower panel) hair cells at a holding potential of -40 mV. **B.** Percentage of maximum response evoked by ACh or choline normalized to the maximal peak response to 3 mM ACh for mouse and chicken hair cells. Values are mean ± S.E.M. of 6 (rat) and 4 (chicken) experiments per group. (*) Friedman's test, vs 3 mM ACh for each species ($p < 0.05$).

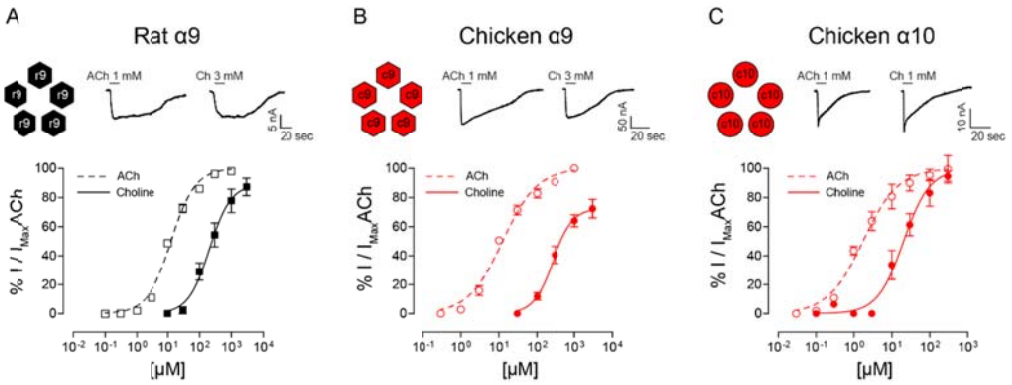

Figure 3. *Responses of rat and chicken homomeric α9 or α10 nAChRs to choline.* Upper panels: representative maximal responses to ACh and choline for rat α9 (A), chicken α9 (B) and chicken α10 (C) homomeric receptors. Lower panels: concentration-response curves for ACh (dotted lines) and choline (solid lines) for rat α9 (A), chicken α9 (B) and chicken α10 (C) homomeric receptors. Values are normalized to the maximal response to ACh obtained in each oocyte. Values are mean ± S.E.M. for 4-6 oocytes.

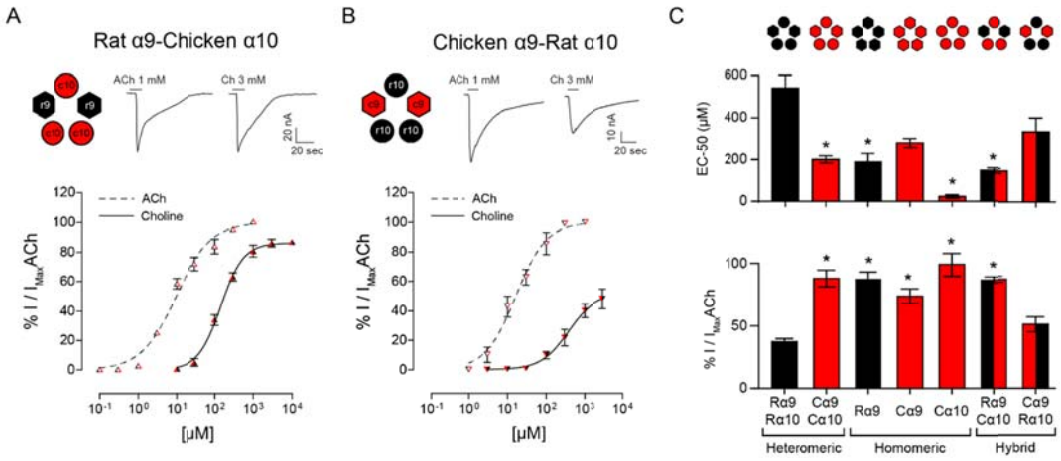

Figure 4. *Responses of rat-chicken hybrid receptors to choline*. A-B. Upper panels: representative maximal responses evoked by saturating concentrations of ACh and choline in rat α9 - chicken α10 (A) and chicken α9 - rat α10 (B) hybrid receptors. Lower panels: concentration-response curves for ACh (dotted lines) and choline (solid lines). Values are normalized to the maximal response to ACh in each oocyte. Values are mean ± S.E.M. of 4-6 oocytes per group. (C) EC_{50} values for choline (Upper panel) and percentage maximal choline response, normalized to the maximal response elicited by ACh (Bottom panel) for rat and chicken heteromeric α9α10 receptors, rat α9, chicken α9 and chicken α10 homomeric receptors, and rat α9 – chicken α10 and chicken α9 – rat α10 hybrid receptors. (*) Kruskal-Wallis test, vs rat α9α10 receptor ($p<0.05$).

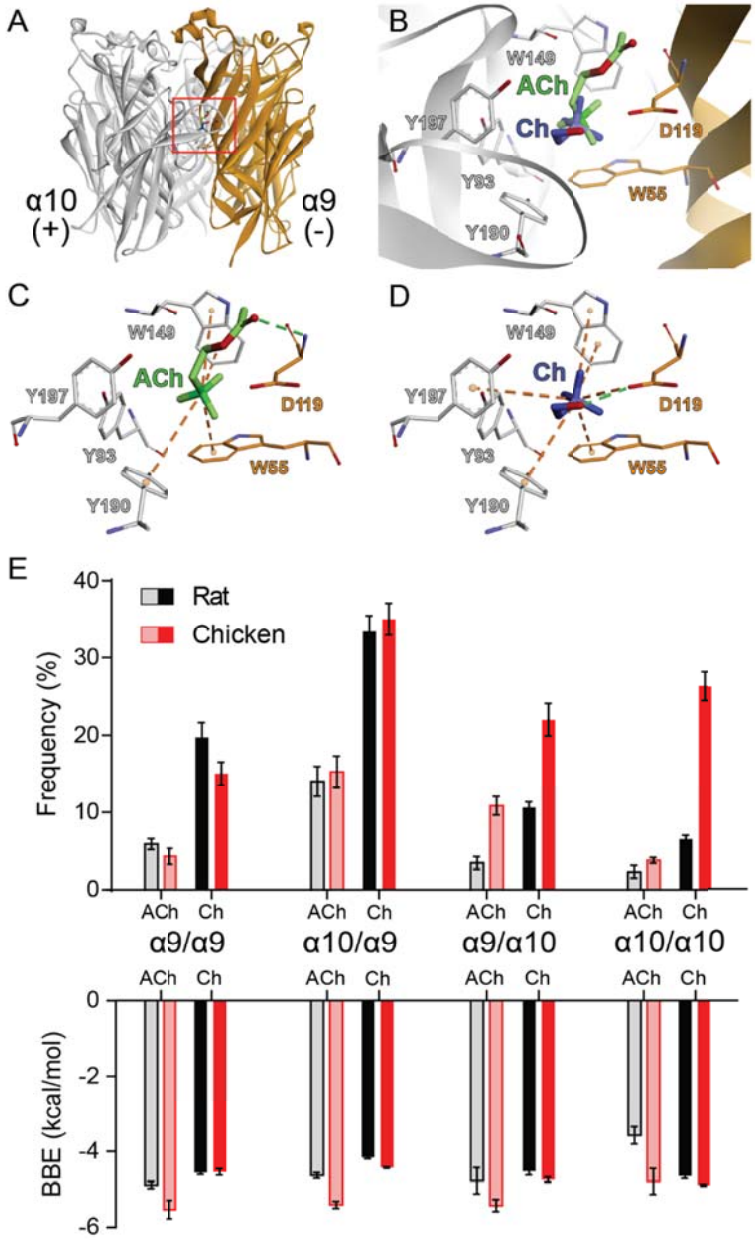

Figure 5. *Docking of ACh and choline into the binding sites of rat and chicken a9a10receptor.* A. Ribbon structure of the extracellular domain of rat α10 and α9 subunits showing an interface formed by the principal (+) component of the α10 subunit and the complementary (-) component of the α9 subunit. The location of the orthosteric binding site with a bound ACh, is highlighted by the red box. B. Zoom in of the binding domain highlighted by the red square in A. The positions of ACh (green) and the most frequent orientation of choline (blue) are shown, docked into the binding. C-D.

874 Molecular interactions of ACh (C) and choline (D) with residues in the binding site.
875 Cation-π interactions are illustrated by orange dashed lines and H-bonds by green
876 dashed lines. E. Frequency (as percentage) of the most frequent orientation (top panel)
877 and best binding energy (BBE; bottom panel) obtained for three separate simulations for
878 ACh and choline in each of the binding interfaces, comprised of
879 (principal/complementary components) α9/α9, α10/α9, α9/α10 and α10/α10 rat or
880 chicken subunits. Values are mean ± SEM of at least three different docking simulations
881 for each interface.

882

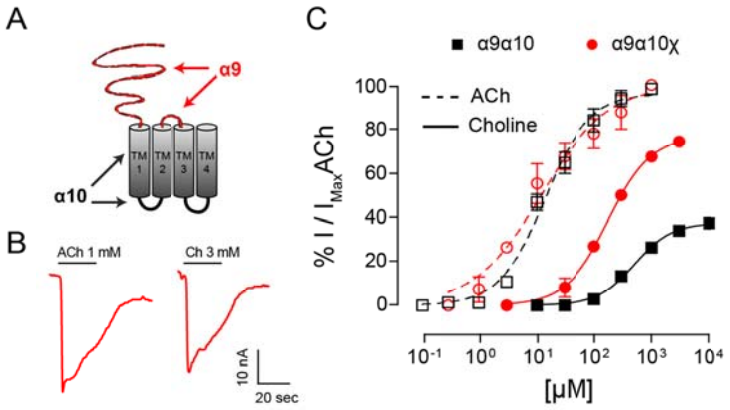

884

892 **Figure 6.** *Responses of rat α9α10$_x$ chimeric receptor to choline*. A. Diagram of a
893 α9α10$_x$ chimeric subunit showing the regions corresponding to the α9 subunit sequence
894 (red) and α10 subunit sequence (black). B. Representative maximal responses to ACh
895 (left) and choline (right) for the α9α10$_x$ chimeric receptor, obtained by co-expressing
896 the α10$_x$ chimeric subunit with rat α9 subunit. C. Concentration response-curves for
897 ACh (dotted lines) and choline (solid liness) for α9α10$_x$ chimeric receptors (red circles)
898 and wild-type α9α10 receptors (black squares). Values were normalized to the maximal
899 response to ACh in each oocyte. Values are mean ± S.E.M. of 5-9 oocytes per group.

893

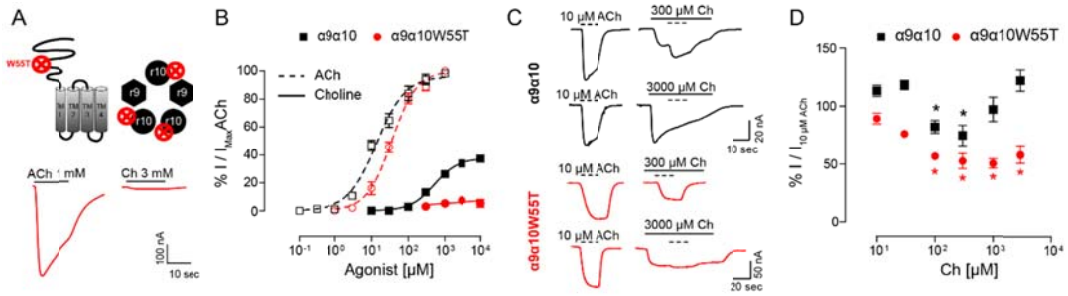

Figure 7. *Responses of the rat α9α10W55T receptor to choline*. A. Diagram of an α10 subunit illustrating the W55T mutation, localized to the complementary component of the agonist binding site within the pentameric assembly (Top panel). Representative maximal responses to ACh (left) and choline (right) for the α9α10W55T receptor (Bottom panel). B. Concentration response-curves to ACh (dotted lines) and choline (solid lines) for the α9α10W55T receptor (red circles) and wild-type α9α10 receptors (black squares). Values were normalized to the maximal response to ACh in each oocyte. Values are mean ± S.E.M. of 5-9 oocytes per group. C. Representative responses to 10 μM ACh (dotted lines) alone or on top of responses to 300 or 3000 μM choline in oocytes expressing rat α9α10 or α9α10W55T receptors. D. Normalized responses to 10 μM ACh obtained in the presence of increasing concentrations of choline for rat α9α10 and α9α10W55T receptors. Responses were normalized to responses to10 μM ACh in the absence of choline for each oocyte.